



The relationship between systolic vector flow mapping parameters and left ventricular cardiac function in healthy dogs

Seijirow Goya¹ · Tomoki Wada¹ · Kazumi Shimada¹ · Daiki Hirao¹ · Ryou Tanaka¹

Received: 30 June 2017 / Accepted: 1 December 2017 / Published online: 11 December 2017
© Springer Japan KK, part of Springer Nature 2017

Abstract

Vector flow mapping (VFM) is a novel echocardiographic technology that shows blood flow vectors and vortexes, enabled the hydrokinetic evaluation of hemodynamics within the left ventricle. VFM provides several unique parameters: circulation, vorticity, vortex area, and energy loss. The present study aims to reveal a relationship between VFM parameters and cardiac function. Five healthy Beagle dogs were anesthetized and administered with dobutamine (0, 2, 4, 8, 12 $\mu\text{g}/\text{kg}/\text{min}$). Pressure–volume diagrams were acquired to assess cardiac function using pressure–volume conductance catheter. Systolic maximum circulation, vorticity, vortex area, and energy loss were measured using VFM. The systolic maximum circulation, systolic vorticity, systolic vortex area, and systolic energy loss were increased by dobutamine administration. There was a strongly significant correlation between the systolic maximum circulation and ejection fraction ($r = 0.76$), maximal positive left ventricular (LV) pressure derivatives (dP/dt max) ($r = 0.80$), and end-systolic LV elastance ($r = 0.73$). Systolic vorticity and systolic vortex area were strongly correlated with ejection fraction ($r = 0.76, 0.68$) and dP/dt max ($r = 0.76, 0.69$), and end-systolic LV elastance ($r = 0.62, 0.74$), respectively. Systolic energy loss was strongly correlated with dP/dt max ($r = 0.78$), systolic maximum circulation ($r = 0.81$), and systolic vorticity ($r = 0.82$). The present study revealed that systolic VFM parameters are associated with the LV contractility. Furthermore, systolic energy loss was susceptible to the systolic vortex parameters such as systolic vorticity and systolic maximum circulation. Systolic VFM parameters are new hydrokinetic indices reflecting LV contractility.

Keywords Echocardiography · Dobutamine stress echocardiography · Left ventricular function · Systolic function · Ultrasound imaging

Introduction

The relationships between intra-ventricular blood flow and cardiac function have been reported recently [1–9] and the assessment of intra-ventricular blood flow is expected to reveal the core of cardiac function. The blood flow visualization methods revealed a vortex occurs during left ventricular (LV) filling and sustains throughout isovolumic contraction period, saving energy for facilitating the blood

ejection into the aorta [5, 9–11]. The most of the studies relating to the intra-ventricular blood flow have discussed about the intra-ventricular blood flow at diastole. Several reports have focused on the systolic intra-ventricular hemodynamics. Zhang et al. [12] reported that the systolic vortex evolution is associated with LV dimensions and functions. However, the properties of the systolic vortex have not yet been elucidated.

Vector flow mapping (VFM) is a new echocardiographic technology that shows blood flow vectors and vortexes using color Doppler and speckle tracking data, thus enabling the hydrokinetic evaluation of hemodynamics within the left ventricle (LV) [1, 4, 13]. VFM allows to measure the intra-ventricular blood flow easily, rapidly, and non-invasively. Recently, circulation and energy loss (EL) become available as the novel quantitative VFM parameters. Circulation, calculated as the integral of vorticity over an area, is defined to quantify the swirling flow inside vortexes within

Electronic supplementary material The online version of this article (<https://doi.org/10.1007/s00380-017-1093-1>) contains supplementary material, which is available to authorized users.

✉ Seijirow Goya
goya@vet.ne.jp

¹ Department of Veterinary Surgery, Faculty of Veterinary Medicine, Tokyo University of Agriculture and Technology, 3-5-8 Saiwai-cho, Fuchu, Tokyo 183-8509, Japan

a scan plane [14]. EL, derived from the velocity vector field of intra-ventricular blood flow, is defined to reflect the efficiency of blood flow [13, 15]. Several reports have proposed the utility of these unique parameters [13, 14, 16]; however, corroborating evidence is still needed to show the significance of these parameters.

Pressure–volume (PV) relations obtained by a conductance catheter have been shown to provide accurate assessments of systolic LV functions. Furthermore, PV loop analysis is optimal to assess the VFM parameters for each cardiac cycle phase.

The objective of the present study is to show the relationship between systolic VFM parameters and cardiac function through PV loop analysis.

Materials and methods

Animals

The five 1- to 2-year-old female Beagle dogs weighing 11.0 ± 2.3 kg (range 8.4–11.7 kg) were evaluated with general physical examination, blood and serum biochemical evaluations, electrocardiography, thoracic radiography, and echocardiography. There was no evidence of abnormalities.

Anesthesia and preparatory procedures

Dogs were premedicated with meloxicam (0.2 mg/kg, SC), atropine sulfate (0.05 mg/kg, SC), buprenorphine hydrochloride (0.01 mg/kg, IV), and midazolam hydrochloride (0.2 mg/kg, IV). Induction was achieved with propofol (4 mg/kg, IV), after that the dogs were intubated and placed in right lateral recumbency. Anesthesia was maintained by administering a mixture of 1.5–2.0% isoflurane and oxygen. The respiratory rate was maintained with a mechanical ventilator. End-tidal CO₂ was monitored and maintained between 35 and 45 mmHg, and heart rate (HR) was recorded using a monitoring instrument. The right femoral artery was catheterized for the measurement of arterial pressure: systolic arterial pressure (SAP), mean arterial pressure (MAP), and diastolic arterial pressure (DAP). A balloon catheter was advanced through the femoral vein to the inferior vena cava under fluoroscopic guidance for vena cava occlusion. PV conductance catheter (Venti-Cath-507; Millar Instruments Inc, Houston, TX) was electronically zeroed at 37 °C and placed into the LV via the left carotid artery under fluoroscopic guidance. The catheter was then connected with the Micro-Tip Pressure Volume System-Ultra Foundation System (MPVS-Ultra-S; ADInstruments, Colorado Springs, CO), PowerLab hardware (ML880 PowerLab 16/30; ADInstruments, Colorado Springs, CO), and LabChart

Pro software (LabChart Pro Upgrade v7; ADInstruments, Colorado Springs, CO).

PV conductance catheter examination

LV end-diastolic and end-systolic volumes (EDV, ESV), ejection fraction (EF), stroke volume (SV), cardiac output (CO) were measured from ten consecutive PV loops, which were recorded and analyzed by LabChart Pro. LV end-diastolic and end-systolic pressure (EDP, ESP), maximal positive LV pressure derivatives (dP/dt max), and stroke work (SW) were also measured. Effective arterial elastance (Ea) was calculated as follows: $Ea = ESP/SV$. End-systolic LV elastance (Ees) was determined using linear regression of the ESP and ESV points from six consecutive PV loops during temporary caudal vena cava occlusion conducted at least three times after HR and SAP returned to the steady state (Fig. 1). Ees and Ea represented the load-independent LV contractility and afterload, respectively. At the end of the experiment, an additional bolus infusion of hypertonic saline was injected to measure the parallel conductance of myocardial tissue. This procedure was necessary for saline calibration and absolute volume conversion [17, 18].

Echocardiographic examination

Echocardiographic examination was performed with a Pro-Sound Alpha 10 ultrasonography system (Hitachi-Aloka Medical, Co. Ltd., Tokyo, Japan), and measurements were recorded at least six times in the left apical five-chamber view. Four consecutive heart-beats were recorded at the end of the expiratory phase. Images for flow visualization were acquired in the cardiac VFM mode, and image width, depth, and spatial–temporal settings were adjusted to obtain the highest possible frame rate while including the whole LV, mitral, and aortic valves in the color-scan area (see supplementary Movie 1). The Nyquist limit for two-dimensional color Doppler imaging was set high enough to decrease aliasing phenomenon.

Vector flow mapping analysis and parameters

Analysis software (DAS-RS1, Hitachi-Aloka Medical, Co. Ltd., Tokyo, Japan) was used to analyze the measurements. Two-dimensional color Doppler images were analyzed with commercially available VFM analysis software to obtain the velocity vector fields of the intra-ventricular hemodynamics. The ventricular endocardial border was manually traced on the beginning frame, and two-dimensional speckle tracking was applied to determine the LV wall motion. After initial manual processing, that is, LV contour definition and aliasing correction, the software upon the detection of a vortex

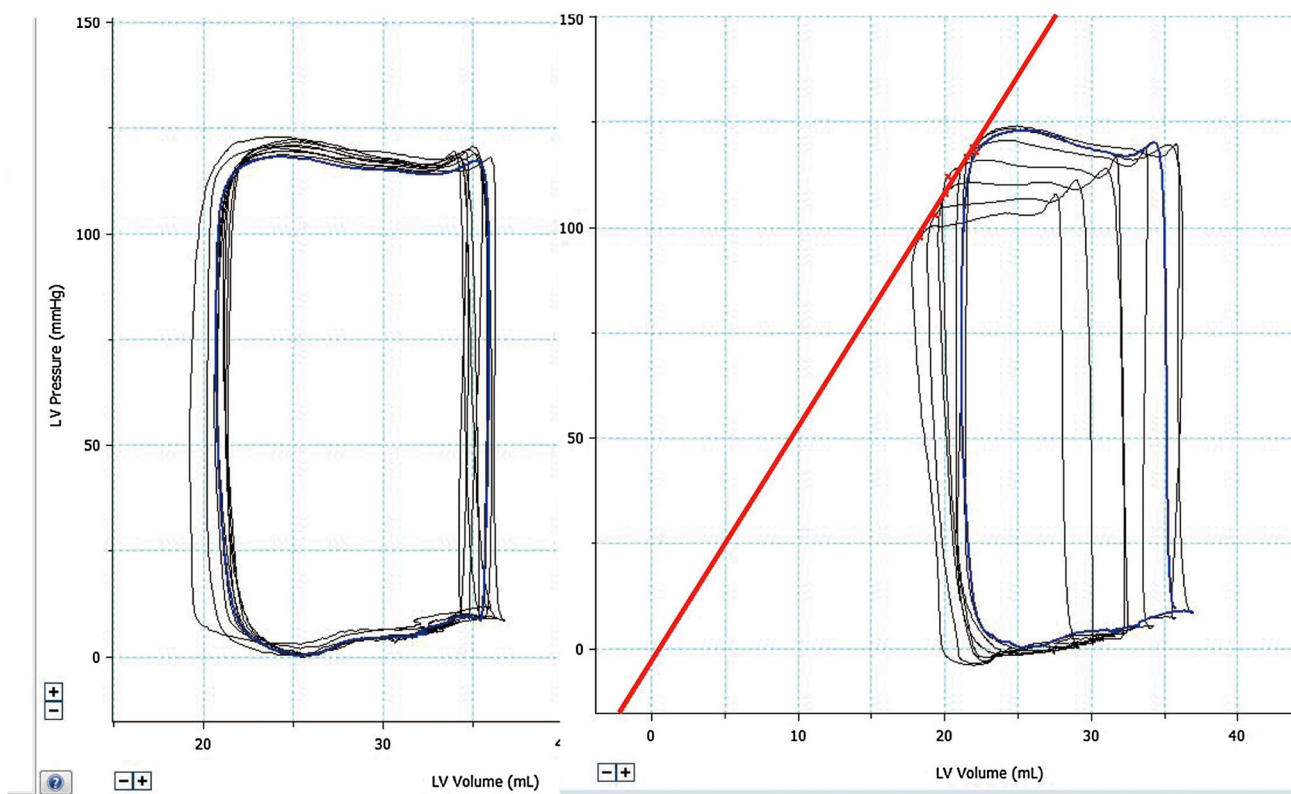


Fig. 1 Left: Steady-state pressure–volume diagrams in the isoflurane-anesthetized healthy dogs. Right: The end-systolic LV elastance (red line) for eight pressure–volume diagram during the inferior vena cava

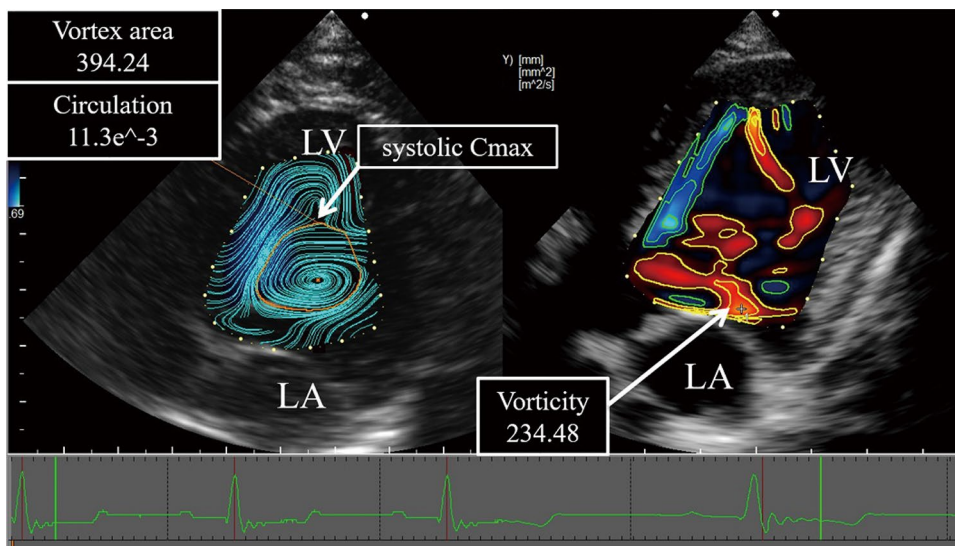
occlusion was used to generate the slope (E_{es}) of the end-systolic pressure–volume relation. *LV* left ventricular

during systole determined the parameters defining circulation and EL.

VFM parameters consist of EL and vortex parameters: circulation, vorticity, and vortex area. Systolic maximum circulation (C_{max}) was a maximum value of circulation from

immediately before aortic valve opening to aortic valve closure. Systolic vortex area was defined as the area at systolic C_{max} . Systolic vorticity was a value of the closest vorticity to the center of the vortex at systolic C_{max} (Fig. 2). Systolic EL within the LV were calculated as the arithmetic means of

Fig. 2 Systolic vorticity was defined as the vorticity closest to the center of the vortex at systolic C_{max} . The left figure shows the systolic C_{max} and vortex area. The right figure shows the systolic vorticity at systolic C_{max} , and the value of systolic vorticity is 234.48 1/s. C_{max} , maximum circulation



the EL during systole [15]. Systolic EL/SW was calculated as energy transfer efficiency from ventricle to blood flow. The systolic vortex formation time corrected by the ejection time (VT/ET) was expressed as the ratio of the frame numbers of the LV vortex existence to all frame numbers during the ejection time [19]. Furthermore, generation timing of systolic C_{\max} that was corrected by ejection timing (GT/ET) was defined as the number of frames from R wave to systolic C_{\max} occurrence per the number of frames of ejection time. To define vortex location, LV was divided into 4 sections by a line from the center of the apex to the mitral-aortic junction and another one perpendicular to the first one at its midpoint [14]. The 4 sections were defined as anterior-basal (AB), posterior-basal (PB), anterior-apical (AAp), and posterior-apical (PAp) and vortex location was registered as the vorticity point located at the frame in which systolic C_{\max} was observed.

Experimental protocol

The cardiovascular measurements including arterial blood pressure measurements and PV loop measurements, and VFM parameters at the baseline loading conditions (BL) were determined after the steady state was maintained with a $2.0 \pm 0.1\%$ end-tidal isoflurane concentration for at least 20 min. Dobutamine was then infused intravenously for $2 \mu\text{g}/\text{kg}/\text{min}$ (at least 10 min). After that the cardiovascular measurements and VFM parameters were measured (DOB2). Dobutamine was successively administered at 4 (DOB4), 8 (DOB8), and 12 (DOB12) $\mu\text{g}/\text{kg}/\text{min}$, and all measurements were collected at each dobutamine level.

Statistical analysis

The results are reported as mean \pm standard deviation (SD). All data were analyzed using the Kruskal–Wallis test and Dunn’s comparisons test. Monolinear regression analysis was conducted to determine the Pearson’s correlation coefficient. Statistical significance was defined as $p < 0.05$. GraphPad Prism (GraphPad Prism version 5.0a, GraphPad, San Diego, CA) was used for the Kruskal–Wallis test, Dunn’s comparisons test, and Monolinear regression analysis.

Reproducibility

To evaluate intra-observer variability, the echocardiography for VFM analysis was repeated in 10 randomly selected conscious Beagle dogs. The repeated analysis was performed a day after the initial analysis. To assess inter-observer variability, the VFM analysis was performed by a second veterinarian. The intra-observer and inter-observer variability were evaluated as the mean percentage error as an absolute difference divided by the mean of the two measurements. A

Bland–Altman analysis of intra-observer and inter-observer variability was also performed for the systolic C_{\max} , vorticity, vortex area, and EL.

Results

Intraventricular blood flow pattern

When LV contractility is low, a large counterclockwise vortex is generated near the anterior leaflet of mitral valve at the early-diastole; this vortex disappeared at the end-diastole without “pinched off”. A systolic vortex was formed in the posterior-basal space from the early-ejection period and remained until the vortex strength reaches the maximum at the end-systole. On the other hand, when LV contractility is high, the large counterclockwise vortex is generated near the anterior leaflet of mitral valve at the early-diastole, which accelerated with atrial kick. The diastolic vortex remained until the isovolumic contraction period but was not “pinched off” from the anterior leaflet of mitral valve. Subsequently, when the aortic valve opened, a large one vortex was generated the entire LV and disappeared rapidly.

Cardiovascular measurements

ESV was significantly decreased at DOB12 compared with that at BL. CO was significantly increased at DOB12 compared with that at BL. EF, dP/dt max, and Ees were significantly increased at DOB8 and DOB12 compared with those at BL. Ea was significantly decreased at DOB8 compared with that at BL. SW was significantly increased at DOB12 compared with that at BL (Table 1).

VFM parameters

Systolic C_{\max} , systolic vorticity, and systolic vortex area were significantly increased at DOB8 and DOB12 compared with those at BL (Table 2). Systolic EL and systolic EL/SW increased significantly at DOB12 compared with those at BL. Regardless of the dobutamine infusion rate, the systolic vortex clearly occurred in the PB region. Systolic C_{\max} was occurred at the late ejection without dobutamine administration; however, it was generated at aortic valve opening as high dose dobutamine administration. The generation timing of systolic C_{\max} changed along with the peak timing of LV pressure (Fig. 3). VT/ET decreased at DOB2 compared with BL and GT/ET decreased at DOB2 or more.

Table 1 Cardiovascular measurements

Parameters	BL	DOB2	DOB4	DOB8	DOB12
HR (bpm)	123 ± 18	117 ± 12	114 ± 14	125 ± 13	158 ± 24
SAP (mmHg)	117 ± 9	118 ± 13	126 ± 13	125 ± 23	129 ± 19
MAP (mmHg)	88 ± 5	85 ± 8	89 ± 8	86 ± 15	89 ± 14
DAP (mmHg)	72 ± 5	69 ± 7	71 ± 9	66 ± 13	67 ± 12
EDV (mL)	31 ± 5	33 ± 5	34 ± 4	30 ± 5	27 ± 5
ESV (mL)	20 ± 4	20 ± 2	19 ± 3	14 ± 3	11 ± 1†
EF (%)	40 ± 6	43 ± 5	47 ± 8	61 ± 6†	65 ± 3‡
SV (mL)	13 ± 3	14 ± 3	16 ± 4	18 ± 3	18 ± 3
CO (L/min)	1.6 ± 0.3	1.7 ± 0.4	1.8 ± 0.5	2.3 ± 0.3	2.9 ± 0.9*
EDP (mmHg)	9 ± 3	10 ± 3	9 ± 3	12 ± 4	12 ± 5
ESP (mmHg)	105 ± 8	104 ± 13	101 ± 15	103 ± 18	104 ± 17
dP/dt max (mmHg/s)	2519 ± 369	2878 ± 790	3140 ± 1141	4889 ± 790†	6076 ± 940‡
Ea (mmHg/mL)	10 ± 2	8 ± 2	6 ± 2	6 ± 2*	7 ± 2
Ees (mmHg/mL)	3.3 ± 0.4	3.8 ± 1.0	5.6 ± 1.7	9.0 ± 3.1†	9.3 ± 2.3†
SW (mmHg mL)	1059 ± 215	1255 ± 376	1404 ± 507	1694 ± 278	1831 ± 323†

Mean ± SD. BL baseline, DOB2 dobutamine 2 µg/kg/min, DOB4 dobutamine 4 µg/kg/min, DOB8 dobutamine 8 µg/kg/min, DOB12 dobutamine 12 µg/kg/min, HR heart rate, SAP systolic arterial pressure, MAP mean arterial pressure, DAP diastolic arterial pressure, EDV end-diastolic volume, ESV end-systolic volume, EF ejection fraction, SV stroke volume, CO cardiac output, EDP end-diastolic pressure, ESP end-systolic pressure, dP/dt max maximal positive LV pressure derivatives, Ea effective arterial elastance, Ees end-systolic LV elastance, SW stroke work

* $p < 0.05$ vs BL. † $p < 0.01$ vs BL. ‡ $p < 0.001$ vs BL

Table 2 VFM parameters

Parameters	BL	DOB2	DOB4	DOB8	DOB12
Systolic C_{max} (m ² /s)	4.4 ± 1.1	5.2 ± 2.6	6.5 ± 3.9	10.3 ± 1.4*	14.6 ± 3.1‡
Systolic vorticity (1/s)	128 ± 17	136 ± 33	175 ± 30	189 ± 21*	273 ± 49‡
Systolic vortex area (mm ²)	114 ± 46	138 ± 52	171 ± 101	269 ± 78*	283 ± 81*
Systolic EL (10 ² N/s)	2.6 ± 0.4	3.9 ± 1.3	3.9 ± 1.8	6.7 ± 2.2	12.8 ± 4.3†
Systolic EL/SW (N/10 ² s mmHg mL)	26.3 ± 7.4	34.0 ± 17.3	27.6 ± 4.8	40.0 ± 11.7	75.4 ± 36.9*
VT/ET	0.55 ± 0.10	0.52 ± 0.07	0.51 ± 0.07	0.47 ± 0.07	0.38 ± 0.04*
GT/ET	0.83 ± 0.04	0.61 ± 0.06*	0.52 ± 0.06*	0.35 ± 0.05*	0.31 ± 0.04*
Vortex location					
(AB/PB)	0/5	0/5	1/4	0/4	0/4
(PAp/AAp)	0/0	0/0	0/0	1/0	1/0

Mean ± SD. BL baseline, DOB2 dobutamine 2 µg/kg/min, DOB4 dobutamine 4 µg/kg/min, DOB8 dobutamine 8 µg/kg/min, DOB12 dobutamine 12 µg/kg/min, C_{max} maximum circulation, EL energy loss, SW stroke work, VT/ET vortex formation time/ejection time, GT/ET generation timing of systolic C_{max} /ejection time, AB anterior-basal, PB posterior-basal, PAp posterior-apical, AAp anterior-apical

* $p < 0.05$ vs BL. † $p < 0.01$ vs BL. ‡ $p < 0.001$ vs BL

Relationship between cardiovascular measurements and vortex parameters

Table 3 showed the correlation between cardiovascular measurements and systolic VFM parameters. There was a strongly significant correlation between the Systolic C_{max} and EF, dP/dt max, and Ees. The systolic C_{max} was increased along with the increase in Ees (Fig. 4). Systolic vorticity was strongly correlated with EF and dP/dt max. Figure 5

showed the correlation between dP/dt max and systolic C_{max} and systolic vorticity. Systolic vortex area was strongly correlated with Ees.

Relationship between EL and cardiovascular measurements, and vortex parameters

The correlations of systolic EL and systolic EL/SW with cardiovascular measurement, systolic C_{max} , vorticity, and

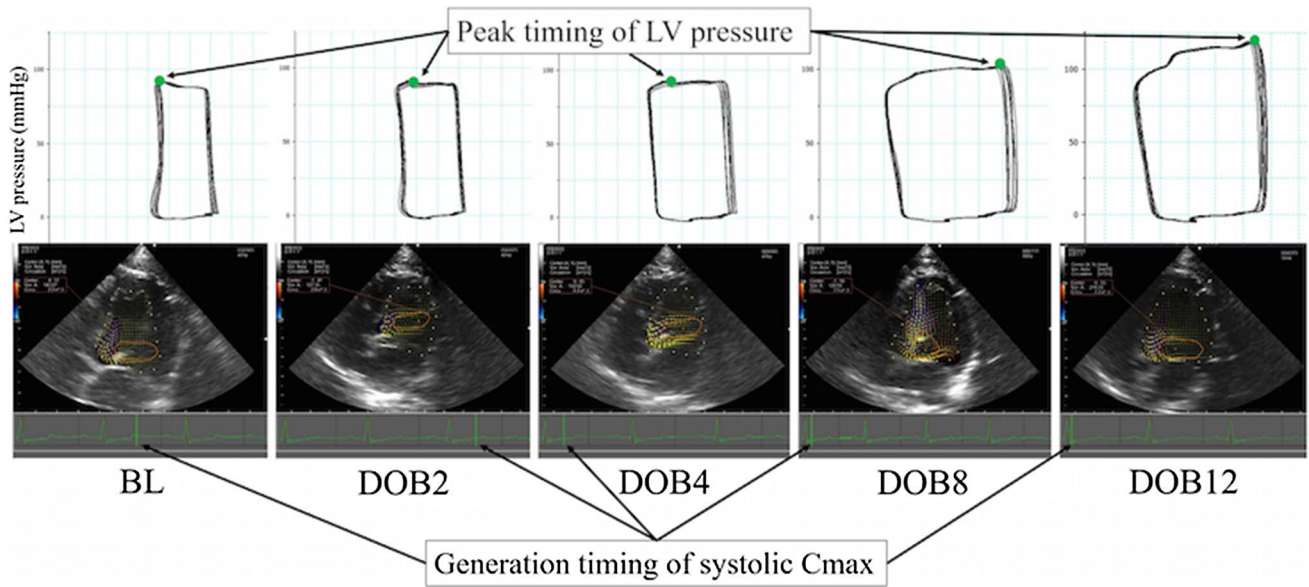


Fig. 3 Relationship between the generation timing of systolic C_{max} and the peak timing of LV pressure. The upper figure shows PV loops and lower figure shows VFM views at systolic C_{max} in each dobutamine infusion rate. Green closed circles on the PV loops shows the

peak timing of LV pressure and green bars on the ECGs in each VFM views shows the generation timing of systolic C_{max} . *BL* baseline; *DOB2* dobutamine 2 $\mu\text{g}/\text{kg}/\text{min}$; *DOB4* dobutamine 4 $\mu\text{g}/\text{kg}/\text{min}$; *DOB8* dobutamine 8 $\mu\text{g}/\text{kg}/\text{min}$; *DOB12* dobutamine 12 $\mu\text{g}/\text{kg}/\text{min}$

Table 3 Correlation between systolic vortex parameters and cardiovascular measurements

	Systolic C_{max}		Systolic vorticity		Systolic vortex area	
	<i>p</i>	<i>r</i>	<i>p</i>	<i>r</i>	<i>p</i>	<i>r</i>
HR	0.0144	0.48	0.0264	0.44	0.0964	–
SAP	0.1340	–	0.0951	–	0.4845	–
MAP	0.2890	–	0.5587	–	0.4005	–
DAP	0.8570	–	0.7150	–	0.7946	–
EDV	0.0616	–	0.4514	–	0.0582	–
ESV	< 0.0001	0.71	0.0005	0.64	0.0004	0.65
EF	< 0.0001	0.76	< 0.0001	0.76	0.0002	0.68
SV	0.0342	0.43	0.0028	0.57	0.0803	–
CO	0.0016	0.59	0.0002	0.68	0.0173	0.47
EDP	0.0433	0.41	0.0522	–	0.0455	0.40
ESP	0.0372	0.42	0.2989	–	0.0858	–
dP/dt max	< 0.0001	0.80	< 0.0001	0.76	0.0001	0.69
Ea	0.4351	–	0.0396	0.41	0.5297	–
Ees	< 0.0001	0.73	0.0009	0.62	< 0.0001	0.74
SW	0.0010	0.62	0.0003	0.66	0.0069	0.53

C_{max} maximum circulation, *HR* heart rate, *SAP* systolic arterial pressure, *MAP* mean arterial pressure, *DAP* diastolic arterial pressure, *EDV* end-diastolic volume, *ESV* end-systolic volume, *EF* ejection fraction, *SV* stroke volume, *CO* cardiac output, *EDP* end-diastolic pressure, *ESP* end-systolic pressure, dP/dt max maximal positive LV pressure derivatives, *Ea* effective arterial elastance, *Ees* end-systolic LV elastance, *SW* stroke work, *r* Pearson correlation coefficient

vortex area were shown in Table 4. Systolic EL was strongly correlated with EF, dP/dt max, systolic C_{max} , and systolic vorticity. Figure 6 showed the correlation between systolic EL and systolic C_{max} , systolic vorticity, and dP/dt max.

Systolic EL/SW was correlated with systolic C_{max} and systolic vorticity.

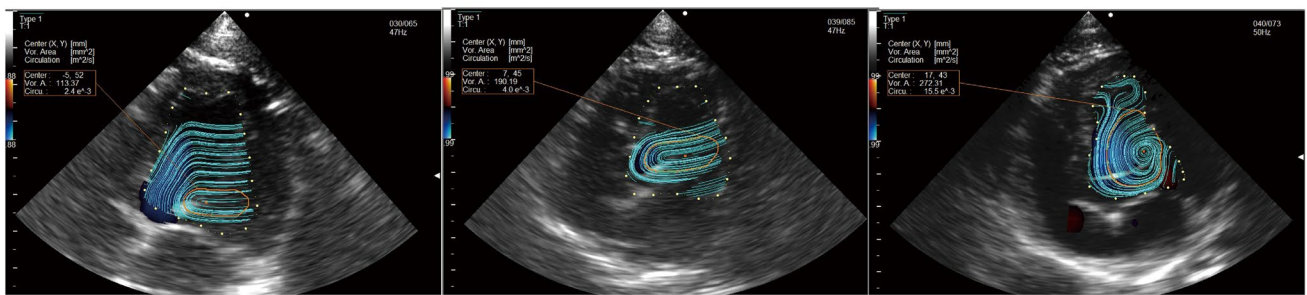
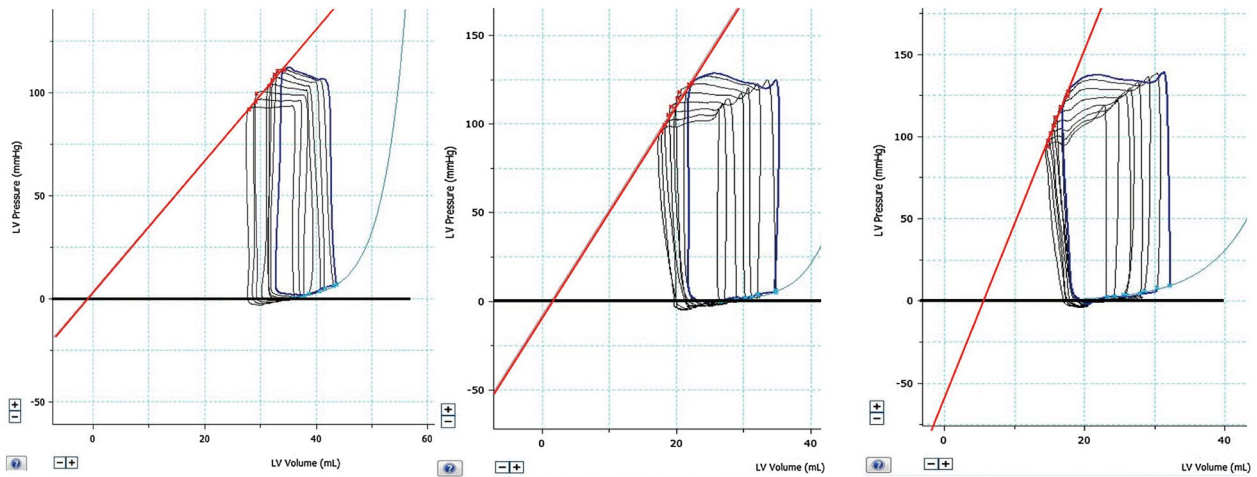
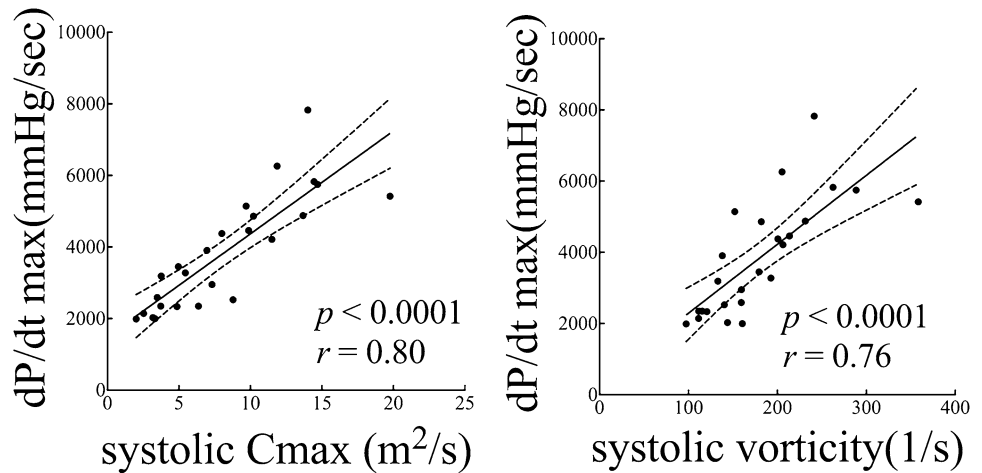


Fig. 4 The figure above shows 8 pressure–volume loop during vena cava occlusion and Ees (red line). The figure below shows the intra-ventricular blood flow patterns during systolic C_{max} . Left: baseline, Center: dobutamine 4 $\mu\text{g}/\text{kg}/\text{min}$, Right: dobutamine 12 $\mu\text{g}/\text{kg}/\text{min}$.

The systolic C_{max} (red circle) was increased along with the increase in Ees caused by dobutamine stress. C_{max} maximum circulation; Ees end-systolic LV elastance

Fig. 5 Relationship between systolic C_{max} and systolic vorticity, and dP/dt max. Strong positive correlations were found between systolic C_{max} and dP/dt max, and between systolic vorticity and dP/dt max. C_{max} = maximum circulation; dP/dt max maximal positive LV pressure derivatives



Reproducibility

Each intra-observer variability for systolic C_{max} , vorticity, vortex area, and EL was 1.6 ± 7.8 , 0.2 ± 11.5 , 2.7 ± 13.0 , and $1.3 \pm 20.6\%$, respectively. Each inter-observer variability for systolic C_{max} , vorticity, vortex area, and EL was

3.2 ± 13.1 , 2.5 ± 14.9 , 1.3 ± 14.5 , and $0.5 \pm 27.2\%$, respectively. Bland–Altman plots of the intra- and inter-observer variability for each systolic VFM parameter are shown in supplemental Figs. 1 and 2. No constant and proportional bias was observed in all parameters.

Table 4 Correlation between Systolic EL and Systolic EL/SW, and Cardiovascular Measurements and Vortex parameters

	Systolic EL		Systolic EL/SW	
	<i>p</i>	<i>r</i>	<i>p</i>	<i>r</i>
HR	0.0950	–	0.1076	–
SAP	0.3665	–	0.6621	–
MAP	0.5453	–	0.8335	–
DAP	0.8820	–	0.4656	–
EDV	0.1301	–	0.0163	0.48
ESV	0.0001	0.70	0.0020	0.59
EF	< 0.0001	0.73	0.3089	–
SV	0.0366	0.42	0.7440	–
CO	0.0088	0.51	0.5848	–
EDP	0.0016	0.60	0.0277	0.44
ESP	0.0452	0.40	0.0756	–
<i>dP/dt</i> max	< 0.0001	0.78	0.0025	0.58
<i>Ea</i>	0.3223	–	0.5323	–
<i>Ees</i>	0.0009	0.62	0.0062	0.53
SW	0.0017	0.59	0.6744	–
Systolic C_{max}	< 0.0001	0.81	0.0020	0.59
Systolic vorticity	< 0.0001	0.82	0.0005	0.64
Systolic vortex area	0.0014	0.60	0.0376	–

EL energy loss, *HR* heart rate, *SAP* systolic arterial pressure, *MAP* mean arterial pressure, *DAP* diastolic arterial pressure, *EDV* end-diastolic volume, *ESV* end-systolic volume, *EF* ejection fraction, *SV* stroke volume, *CO* cardiac output, *EDP* end-diastolic pressure, *ESP* end-systolic pressure, *dP/dt* max maximal positive LV pressure derivatives, *Ea* effective arterial elastance, *Ees* end-systolic LV elastance, *SW* stroke work, C_{max} maximum circulation, *r* Pearson correlation coefficient

Discussion

Our study indicated that the strength of systolic vortex was associated with the LV contractility. Several blood flow visualization studies have focused on the relationship between the systolic vortex and systolic function. These reports have not been compared with PV loop analysis, and the relevance between LV contractility and vortex index has not been clarified [12, 19]. Systolic C_{max} was correlated strongly with *dP/dt* max and *Ees*, which was suggested the quantitative vortex index enables to assess LV contractility. EF shows LV strain, which is just a deformation affected by stress, but does not mean LV contractility such as *Ees* and *dP/dt* max. The quantitative evaluation of LV contractility in the clinical scene is very important. For example, lower *dP/dt* max, not EF, independently predicts cardiac mortality or heart failure hospitalization in patients receiving CRT [20].

Shortening and lengthening of the LV wall results in rotary movements due to the spiral geometry of the myofibers. During isovolumic contraction period, shortening of the subendocardial fibers and stretching of the subepicardial fibers result in a brief clockwise rotation of the apex [22, 23]. During ejection period, the direction of rotation is mainly governed by the subepicardial fibers [24, 25]. Shortening of subepicardial fibers results in anticlockwise rotation of the LV apex and clockwise rotation of the LV base, eventually causes a torsion. This continuous rotational motion may be a factor that generates the systolic vortex by imparting a helical directionality to the fluid within the LV. This shows the physiological relevance between LV contractility and systolic vortex. In our study, LV torsion could not be obtained since the short-axis view was not recorded. Therefore, it was impossible to directly discuss the relationship between the LV torsion and systolic vortex strength. Lee et al. [26]

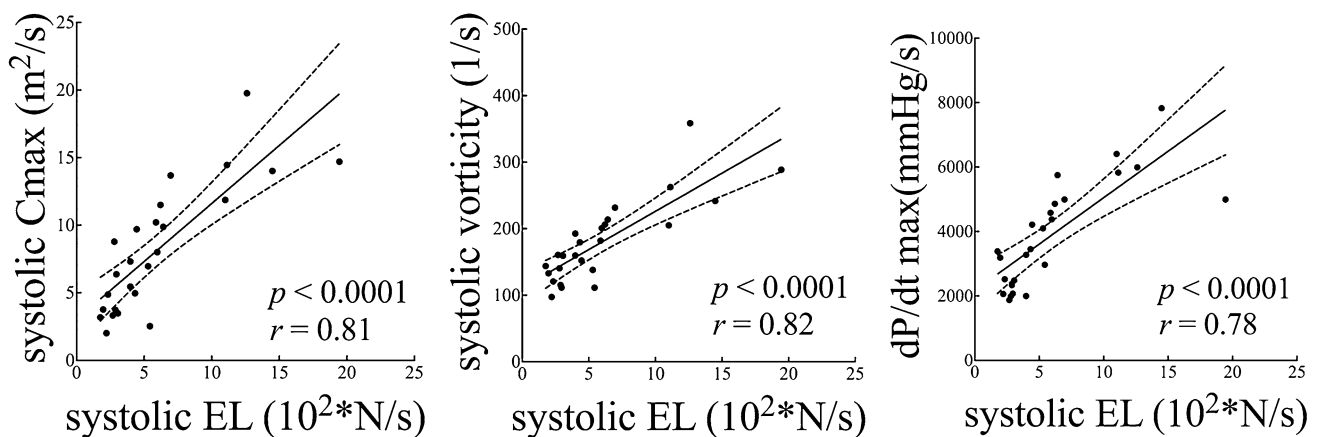


Fig. 6 Relationship between systolic C_{max} , systolic vorticity, *dP/dt* max, and systolic EL. Strong positive correlations were found between systolic EL and systolic C_{max} , systolic vorticity, and *dP/dt*

dt max. C_{max} maximum circulation; *dP/dt* max maximal positive LV pressure derivatives; EL = energy loss

demonstrated that the LV torsion correlates with the LV contractility. It is assumed that there is strong correlation between the LV torsion and the systolic vortex strength. Further research has been expected for the direct relationship between LV torsion and systolic vortex strength.

Circulation, which expressed the strength of a vortex, was defined as the integral of vorticity over a vortex area. In our study, increasing in both systolic vorticity and systolic vortex area eventually increased systolic C_{\max} . Vorticity is a mathematical term that physically corresponds to twice the local angular velocity of a fluid particle, and develops in the form of a shear layer adjacent to the tissue as a consequence of the velocity difference between the solid boundary and the flow [27]. With high dose dobutamine administration, a rapid LV wall movement will cause a rapid rise of LV pressure. The large velocity difference between the LV wall and the intra-ventricular fluid will increase the systolic vorticity. This may be the reason why there is strong correlation between systolic vorticity and dP/dt max. Systolic vortex area was also related to the LV contractility, namely Ees which was a load-independent contractility index. Systolic vortex area increased along with cardiac contractile in our study, while Zhang et al. [4] claimed vortex area during systole increases in patients with low cardiac contractile. Another study revealed the difference of the vortex area between normal subjects and patients with abnormal LV systolic function [28]. The diastolic vortex area is affected from intra-ventricular size [29]. Systolic vortex area may be affected not only from LV contractility but also from intra-ventricular size. Since Ees is also affected by LV size, this similarity may be contributed to the high correlation between Ees and systolic vortex area. Our study showed that systolic vortex area is increased by inotropic agents at least in healthy heart though the influence of the heart size could not be clarified. According to the above reasons, the systolic vortex area should be carefully interpreted.

The duration of systolic vortex was shortened as the LV contractility increased with dobutamine stress. Additionally, the generation timing of systolic C_{\max} was shifted by dobutamine stress from the end-systole to the early-systole, which changed along with the peak timing of LV pressure. These results can explain by the characteristics of the vorticity and the vortex area. In the case of low LV contractility, the LV pressure and vorticity peaks at the end-systole, and there is posterior-basal space sufficient to form a vortex even at the end-systole due to the large ESV. Therefore, small vortex generated from the early-systole continues until the end-systole, eventually C_{\max} occurs at the end-systole. On the other hand, in the case of high LV contractility, since the LV pressure and vorticity peak at the aortic valve opening in addition to the large LV space near the isovolumic contraction period, C_{\max} occurs immediately after the aortic valve opening. As the LV wall contracted, the posterior-basal space

became rapidly so small that the vortex could not remain, and the vortex was absorbed with the outflow stream. For the above reasons, it is considered that the vortex formation time is prolonged at low LV contractility and shortened at high LV contractility. These findings revealed the relationship between vortex formation time and LV contractility and suggested that systolic C_{\max} is useful for estimating LV pressure peak timing. When the peak of LV pressure changes from early-systole to late-systole, that is, when loading sequence changes, energy efficiency and LV isovolumic relaxation deteriorate [21]. The generation timing of systolic C_{\max} may be clinically useful to clarify the change of this loading sequence.

Our results that the vortex strength was correlated with LV contractility and systolic EL/SW suggested that myocardium kinetic energy is converted into the systolic vortex strength, which power is utilized to pump from the heart to the systemic organs. Systolic EL means “systolic hydrokinetic energy” and SW means “mechanical external work of the myocardium”. Therefore, systolic EL/SW is considered to represent “the ratio of fluid energy to generated myocardial mechanical work”. It is the nature of cardiac function that the energy transfer from the myocardium (solid) to the blood (fluid). Only the movement of the cardiac wall and/or a part of the blood flow has been assessed by the conventional echocardiography. This study revealed that the VFM allows to evaluate the whole movement of blood flow within the LV caused by systolic wall motion in terms of the hydrokinetics and the systolic vortex indices (systolic C_{\max} , systolic vorticity) represent energy efficiency of ventricular blood flow performance. A role of systolic vortex is to impart a specific direction and a force to the blood flow through the aorta. A right-handed helix is observed in the aorta, and distortion of the helical blood flow is associated with cardiovascular disease and renal function deterioration [30, 31]. There are few papers reporting the relationship between the systolic vortex and the aortic helix flow, but it is considered that they are not irrelevant. If an abnormality occurs in the systolic vortex, the distortion may also occur in the helical blood flow through the aorta, eventually will induce the various cardiovascular diseases.

The present study also revealed that systolic EL is influenced by the systolic vorticity and circulation. EL represents the dispersion of blood flow vector such as vortex and turbulence, and increases as total fluid energy increases. Many studies have addressed the characteristics of EL [13, 15, 16, 32]; however, few studies have focused on the relationship between EL and vortex parameters. The enhanced LV contractility by dobutamine stress increased the vortex parameters during systole, resulting in the rise of systolic EL in healthy heart. If systolic vortex is used for the ejection energy, the increase in systolic EL does not necessarily mean inefficient energy transfer. When EL is used in clinical

scene, it is important which of the vortex and turbulence contributed to the increase in EL. As in our study, it seems clinically desirable that the increase in EL associated with the increase in vortex energy. However, the increase in EL without the rise of vortex energy implies the rise of turbulence, which is inefficient to the total fluid energy generated. EL alone cannot clarify whether the increase in EL is desirable clinically, but allows to evaluate hydrokinetic balance within the LV by using it together with a vortex indices. These findings show that we must consider the effects of the systolic vortex parameters on systolic EL. Hayashi et al. [15] reported the systolic EL is affected by HR and eventually associated with LV contractility caused by the force-frequency effect. In our study, the correlation between systolic EL and HR was not observed. The increasing in systolic EL was more related to the increase in LV contractility rather than the rise of HR. These results were consistent with a report that EL is associated with dP/dt in patients with Fontan circulation [32]. In addition to this clinical report, our study revealed that the increasing in LV contractility increases systolic vorticity and circulation, eventually causes to elevate the systolic EL in healthy heart. Elevation of systolic EL in clinical field may be not necessarily meaning the degradation of energy efficiency, and vortex indices should also be measured simultaneously to reveal the clinical implication of EL.

Limitations

The present study has several limitations. First, the presence of PV catheter in LV cavity may have affected the intra-ventricular blood flow and vortex within the LV. The catheter may be disturbed intra-ventricular blood flow and/or generate aberrant vortex. However, in our experiment, there was little effect on intraventricular blood flow due to the presence or absence of catheter. Since the catheter was inserted along the LV wall, the influence on the VFM parameters was considered to be negligible. Second, the dogs in this study were under anesthesia, and we could not exclude the possibility of the anesthetic effect on the VFM parameters. Third, the temporal resolution of the VFM analysis was dependent on the frame rate of the two-dimensional color Doppler echocardiography. In this study, the frame rate was adjusted in the range of 47–50 Hz according to HR. Although significant difference in HR under dobutamine stress was absent in our study, the color Doppler cine loops consisted of 9–13 frames per systolic phase, which might be unsuitable to evaluate the peak EL during systole. We used the arithmetic means of the EL during systole, which were less affected by the low frame rate. Fourth, not only the systole but also the

diastolic external work is included in the results, since SW represents the external work in a whole cardiac cycle. It is not possible to separate SW accurately into systolic and diastolic external work. Additionally, the problem about the difference in 2D or 3D physical quantity between EL and SW is also one of the limitations. Fifth, we performed only dobutamine stress in the present study, and have to do additional experiments in various conditions. Although no high correlations observed between systolic VFM parameters and afterload (E_a) and preload (EDV and EDP), it is necessary to investigate how the VFM parameters change when only the preload or afterload is changed. Finally, our study was unable to clarify the difference of systolic vortex parameters between patients with systolic or diastolic dysfunction and healthy subjects. Using our findings, however, we can speculate the difference between systolic vortex parameters of systolic dysfunction patients and those of healthy subjects. For example in patients with dilated cardiomyopathy, it is expected that the decrease in systolic vorticity and the increase in systolic vortex area due to the decrease in the LV contractility and the increase in the ESV. Furthermore, systolic vortex duration may be prolonged in systolic dysfunction patients due to the increase in the ESV. In fact, several reports documented that the systolic vortex formation time of patients with systolic dysfunction is prolonged [12, 19]. Additionally, in patients with diastolic dysfunction such as HFpEF, since EF and LV contractility are maintained, the systolic C_{max} , systolic vorticity, and systolic vortex area are not likely to be different from healthy subjects. However, since systolic C_{max} and systolic vorticity were related to the changes in pressure (dP/dt_{max}), it is expected that vorticity and circulation in diastole may be related to diastolic function such as intraventricular pressure difference and dP/dt_{min} . Recently intracardiac blood flow dynamics of patients with diastolic dysfunction has attracted a lot of attention. In the present study, we focused only on the systolic vortex parameters; however, future studies investigating the characteristics of diastolic vortex parameters will enable to evaluate the detailed pathology of patients with diastolic dysfunction.

Conclusions

The present study showed the relationship between systolic VFM parameters in the LV cavity and the LV contractility. These findings can be used in future studies examining patients with heart disease and it is helpful to understand the intra-ventricular hemodynamic in terms of hydrokinetic.

Compliance with ethical standards

Conflict of interest The authors declare that there is no conflict of interest.

Funding This research received no specific Grant from any funding agency in the public, commercial, or not-for-profit sectors.

Ethical approval During the study, the dogs were managed and cared for in accordance with the standards established by the Tokyo University of Agriculture and Technology (TUAT) and described in its “Guide for the Care and Use of Laboratory Animals”. This study was approved by the Experimental Animal Committee of TUAT (Acceptance No. 26-95).

Appendix

$$\text{“Vorticity } (\omega) = \begin{pmatrix} \frac{\partial w}{\partial y} - \frac{\partial v}{\partial z} \\ \frac{\partial u}{\partial z} - \frac{\partial w}{\partial x} \\ \frac{\partial v}{\partial x} - \frac{\partial u}{\partial y} \end{pmatrix},$$

u, v, w is the velocity components in x, y, z axes directions, respectively.

In 2D flow with $w = 0$,

$$\text{Vorticity } (\omega) = \frac{\partial v}{\partial x} - \frac{\partial u}{\partial y}$$

$$\text{“Circulation} = \iint_S \omega_n dS\text{”}$$

S is the arbitrary curved surface surrounded by a closed curve; ω_n is the normal component of vorticity ω .

$$\begin{aligned} \text{“Energy loss} &= \int \mu \frac{1}{2} \sum_{ij} \left(\frac{\partial u_i}{\partial x_j} + \frac{\partial u_j}{\partial x_i} \right)^2 dv \\ &= \mu \int \left(2 \frac{\partial u^2}{\partial x} + \left(\frac{\partial u}{\partial y} + \frac{\partial v}{\partial x} \right)^2 + 2 \frac{\partial v^2}{\partial y} \right) dv \end{aligned}$$

μ is the coefficient of blood viscosity; u, v is the velocity components in x, y axes directions, respectively.

References

- Lu J, Li WH, Zhong Y, Luo AG, Xie SH, Yin LX (2012) Intuitive visualization and quantification of intraventricular convection in acute ischemic left ventricular failure during early diastole using color Doppler-based echocardiographic vector flow mapping. *Int J Cardiovasc Imaging* 28:1035–1047
- Baccani B, Domenichini F, Pedrizzetti G, Tonti G (2002) Fluid dynamics of the left ventricular filling in dilated cardiomyopathy. *J Biomech* 35:665–671
- Loerakker S, Cox LGE, van Heijst GJF, de Mol BAJM, van de Vosse FN (2008) Influence of dilated cardiomyopathy and a left ventricular assist device on vortex dynamics in the left ventricle. *Comput Methods Biomech Biomed Eng* 11:649–660
- Zhang HB, Zhang J, Zhu XX, Chen LL, Liu LW, Duan YY, Yu M, Zhou XD, Zhu T, Zhu MZ, Li HL (2012) The Left Ventricular intracavitary vortex during the isovolumic contraction period as detected by vector flow mapping. *Echocardiography* 29:579–587
- Kheradvar A, Houle H, Pedrizzetti G, Tonti G, Belcik T, Ashraf M, Lindner JR, Gharib M, Sahn D (2010) Echocardiographic particle image velocimetry: a novel technique for quantification of left ventricular blood vorticity pattern. *J Am Soc Echocardiogr* 23:86–94
- Ohtsuki S, Tanaka M (2006) The flow velocity distribution from the Doppler information on a plane in three-dimensional flow. *J Visual Jpn* 9:69–82
- Mehregan F, Tournoux F, Muth S, Pibarot P, Rieu R, Cloutier G, Garcia D (2014) Doppler vortography: a Color Doppler approach to quantification of intraventricular blood flow vortices. *Ultrasound Med Biol* 40:210–221
- Kvitting JPE, Ebberts T, Wigstrom L, Engvall J, Olin CL, Bolger AF (2004) Flow patterns in the aortic root and the aorta studied with time-resolved, 3-dimensional, phase-contrast magnetic resonance imaging: implications for aortic valve-sparing surgery. *J Thorac Cardiovasc Surg* 127:1602–1607
- Ishizu T, Seo Y, Ishimitsu T, Obara K, Moriyama N, Kawano S, Watanabe S, Yamaguchi I (2006) The wake of a large vortex is associated with intraventricular filling delay in impaired left ventricles with a pseudonormalized transmitral flow pattern. *Echocardiography* 23:369–375
- Kheradvar A, Gharib M (2009) On mitral valve dynamics and its connection to early diastolic flow. *Ann Biomed Eng* 37:1–13
- Kheradvar A, Milano M, Gharib M (2007) Correlation between vortex ring formation and mitral annulus dynamics during ventricular rapid filling. *ASAIO J* 53:8–16
- Zhang H, Liu L, Chen L, Ma N, Zhou L, Liu Y, Li Z, Liu C, Hou R, Zhu S (2013) The evolution of intraventricular vortex during ejection studied by using vector flow mapping. *Echocardiography* 30:27–36
- Itatani K, Okada T, Uejima T, Tanaka T, Ono M, Miyaji K, Takenaka K (2013) Intraventricular flow velocity vector visualization based on the continuity equation and measurements of vorticity and wall shear stress. *Jpn J Appl Phys* 52:07HF16
- Munoz DR, Mur JLM, Fernandez-Golfín C, Becker DC, Gomez A, Santos SF, Rivera CL, Diaz LMR, Rojo EC, Gomez JLZ (2015) Left ventricular vortices as observed by vector flow mapping: main determinants and their relation to left ventricular filling. *Echocardiography* 32:96–105
- Hayashi T, Itatani K, Inuzuka R, Shimizu N, Shindo T, Hirata Y, Miyaji K (2015) Dissipative energy loss within the left ventricle detected by vector flow mapping in children: normal values and effects of age and heart rate. *J Cardiol* 66:403–410
- Garcia D, Pibarot P, Dumesnil JG, Sakr F, Durand LG (2000) Assessment of aortic valve stenosis severity—a new index based on the energy loss concept. *Circulation* 101:765–771
- Baan J, van der Velde ET, de Bruin HG, Smeenk GJ, Koops J, van Dijk AD, Temmerman D, Senden J, Buis B (1984) Continuous measurement of left ventricular volume in animals and humans by conductance catheter. *Circulation* 70:812–823
- Steendijk P, Staal E, Jukema JW, Baan J (2001) Hypertonic saline method accurately determines parallel conductance for dual-field conductance catheter. *Am J Physiol-Heart Circ Physiol* 281:H755–H763
- Fukuda N, Itatani K, Kimura K, Ebihara A, Negishi K, Uno K, Miyaji K, Kurabayashi M (2001) Takenaka K (2014) Prolonged vortex formation during the ejection period in the left ventricle with low ejection fraction: a study by vector flow mapping. *J Med Ultrasonics* 41:301–310

20. Suzuki H, Shimano M, Yoshida Y, Inden Y, Muramatsu T, Tsuji Y, Tsuboi N, Hirayama H, Shibata R, Murohara T (2010) Maximum derivative of left ventricular pressure predicts cardiac mortality after cardiac resynchronization therapy. *Clin Cardiol* 33:E18–E23
21. Kohno F, Kumada T, Kambayashi M, Hayashida W, Ishikawa N, Sasayama S (1996) Change in aortic end-systolic pressure by alterations in loading sequence and its relation to left ventricular isovolumic relaxation. *Circulation* 93:2080–2087
22. Sengupta PP, Khandheria BK, Korinek J, Wang J, Jahangir A, Seward JB, Belohlavek M (2006) Apex-to-base dispersion in regional timing of left ventricular shortening and lengthening. *J Am Coll Cardiol* 47:163–172
23. Kroeker CA, Tyberg JV, Beyar R (1995) Effects of ischemia on left ventricular apex rotation. An experimental study in anesthetized dogs. *Circulation* 92:3539–3548
24. Taber LA, Yang M, Podszus WW (1996) Mechanics of ventricular torsion. *J Biomech* 29:745–752
25. Davis JS, Hassanzadeh S, Winitsky S, Lin H, Satorius C, Vemuri R, Aletras AH, Wen H, Epstein ND (2001) The overall pattern of cardiac contraction depends on a spatial gradient of myosin regulatory light chain phosphorylation. *Cell* 107:631–641
26. Kim WJ, Lee BH, Kim YJ, Kang JH, Jung YJ, Song JM, Kang DH, Song JK (2009) Apical rotation assessed by speckle-tracking echocardiography as an index of global left ventricular contractility. *Circ Cardiovasc Imaging* 2:123–131
27. Sengupta PP, Pedrizzetti G, Kilner PJ, Kheradvar A, Ebberts T, Tonti G, Fraser AG, Narula J (2012) Emerging trends in CV flow visualization. *JACC Cardiovasc Imaging* 5:305–316
28. Hong GR, Pedrizzetti G, Tonti G, Li P, Wei Z, Kim JK, Baweja A, Liu S, Chung N, Houle H, Narula J, Vannan MA (2008) Characterization and quantification of vortex flow in the human left ventricle by contrast echocardiography using vector particle image velocimetry. *JACC Cardiovasc Imaging* 1:705–717
29. Bot H, Verburg J, Delemarre BJ, Strackee J (1990) Determinants of the occurrence of vortex rings in the left-ventricle during diastole. *J Biomech* 23:607–615
30. Houston JG, Gandy SJ, Sheppard DG, Dick JB, Belch JJ, Stonebridge PA (2003) Two-dimensional flow quantitative MRI of aortic arch blood flow patterns: effect of age, sex, and presence of carotid atheromatous disease on prevalence of spiral blood flow. *J Magn Reson Imaging* 18:169–174
31. Houston JG, Gandy SJ, Milne W, Dick JB, Belch JJ, Stonebridge PA (2004) Spiral laminar flow in the abdominal aorta: a predictor of renal impairment deterioration in patients with renal artery stenosis? *Nephrol Dial Transplant* 19:1786–1791
32. Honda T, Itatani K, Takanashi M, Mineo E, Kitagawa A, Ando H, Kimura S, Nakahata Y, Oka N, Miyaji K, Ishii M (2014) Quantitative evaluation of hemodynamics in the fontan circulation: a cross-sectional study measuring energy loss in vivo. *Pediatr Cardiol* 35:361–367